Spin transport and spin dynamics in antiferromagnets

Hoogeboom, Geert

DOI:
10.33612/diss.157444391

Chapter 3

Experimental methods

3.1 Abstract

While Ch. 2 discussed the theoretical background to understand the research performed in this thesis, this methods chapter discusses the way the samples were fabricated and how the measurements are performed. For the creation of spin currents, thin films of Pt are deposited on the various studied magnets. This part of the device fabrication has been previously employed and described in the *Physics of Nanodevices* (FND) group [1–4] and carried out in the clean room Groningen of the NanoLabNL consortium. The best way to learn these methods is by a daily supervisor or discussions with people, but in written form this could still be of interest for beginning PhDs and students who are just beginning their research or as an inspiration for other groups working in similar fields. The magnetic properties of the magnetic insulators studied in this thesis are described in their respective chapters.

Relevant information is provided in Sec. 3.2 regarding the work performed on the samples in Groningen such as establishing the crystallographic direction and the device fabrication techniques, including polishing and the different steps used for patterning the device structures by electron-beam lithography, followed by the description of the used deposition techniques: electron-beam evaporation and sputtering. Further, Sec. 3.3 discusses some basics regarding the measurement technique including the harmonics of the obtained measurement signals.

3.2 Sample fabrication

The magnetic crystals studied in this thesis are of different origin. Many magnetic applications work with thin films. Even though SMR is a surface effect, we preferred to work with bulk materials for these first explorative studies. Substrate induced strain, defects and atomic substitution are interesting effects to study, but our goal was initially to prove the effectiveness of the SMR and SSE in AFMs. A secondary goal was to characterize these materials both for gaining knowledge about these materials and to affirm and relate the acquired data to data acquired with other methods. Therefore, we chose to perform measurements mostly on bulk AFMs.

Chapter 7 is the exception as the goal was to measure the transmissivity of thin AFM films as well as the effects of exchange bias and disorder. These spin currents will be affected by controlling the AFM order by the exchange bias of the adjacent YIG layer. These 260 nm thick YIG samples are commercially obtained from Matesy GmbH and the Unisersité de Bretagne Occidentale in Brest, France. The YIG is grown on GGG substrates with a crystallographic orientation of (111) by liquid phase epitaxy [5]. The NiO thin films in Ch. 7 were grown by Olga Kuschel and Andreas Alexander and the XRR images are performed by Olga Kuschel in the same group of Joachim Wollschläger in Osnabrück University. TEM images are performed by Inga Ennen in the group of Timo Kuschel in Bielefeld University. The fabrication steps in Groningen are described below.

- **X-ray diffraction or x-ray reflectivity**: For a proper surface cut, the crystallographic directions for $DyFeO_3$ have been determined via single-crystal X-ray diffraction and, thereafter these direction are marked onto the crystal. The thin films of NiO of the NiO|YIG samples were investigated by X-ray reflectivity in order to determine their exact thicknesses as discussed in Ch. 7.
- **Polishing**: After the crystallographic axes determination, the crystal was cut by a diamond powdered wire and afterwards glued on a polishing device in order to align the axes to the polished surface. The first polishing step is performed by hand with sandpaper of degreasing grain sizes once the right dimensions have been established. To further reach the required nm RMS roughness the particle size has to be lowered, a DP-Lubricant with diamond powder of subsequently smaller sizes is used on MD-Largo and then a MD-DAC cloth. The later step is performed with the suspension OP-AN with AlO_x particles of 20 nm on a MD-Chem cloth, after which the suspension is thoroughly washed away with water as to get rid of any particles on the surface. Thereafter, the sample is washed and checked with a microscope for any leftover

particles, cracks or other inhomogeneities. A surface roughness of sub-nm has been reached with this technique.

An effort has been made to automate the last part of the polishing process. The Struers polishing apparatus can be programmed and to fit in, the crystal was mounted in a cylinder of resin. However, when measuring SMR to analyze the spin-mixing conductance, the signal was a few orders of magnitude smaller than by using the technique described above. It could be that the resin, being softer than the crystal, attached to the surface, thereby, lowering the spin-mixing conductance.

- **Electron-beam lithography**: In the NanoLabNL, the electron-beam lithography (EBL) was performed which consisted of the following steps.

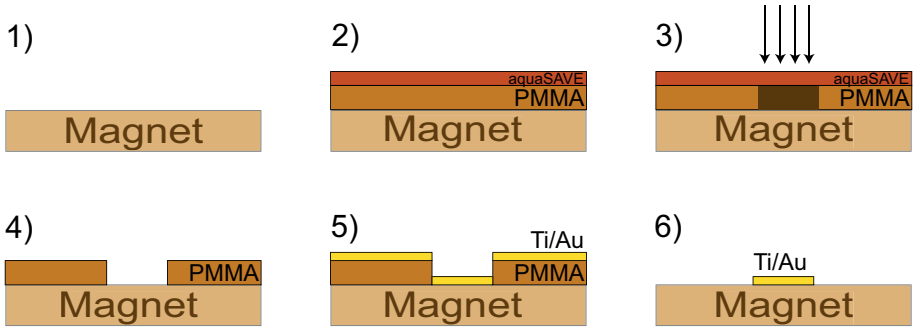

Figure 3.1

1. **Sample cleaning**: After the polishing, performed outside of the cleanroom in a dusty environment, the substrate has to be cleaned. Firstly, the sample is submerged in a beaker containing acetone of 48°, after which it was rinsed with IPA a blow dried with nitrogen to avoid stains. In case of a large amount of dust or polishing particles, sonication was used at low power.
2. **Resist spinning**: At ambient conditions, the adsorption of molecules can cause a lowered spin-mixing conductance at a Pt|magnet interface. Therefore, the sample is heated on a hotplate at 180° C for 90 s. Right after the bake, a layer of positive resist containing 4% PMMA of 950 K (polymethyl methacrylate) dissolved in ethylactate is spin coated at 4000 RPM. The PMMA is sensitive to an electron beam causing the polymer chains to become shorter. While the long chains do not dissolve in the development solution, the exposed area containing the shorter chains has enlarged sol-

ubility. A second heating step of 90 s at 180° removes the solvent, leaving behind a 270 nm thick PMMA layer.

To avoid electrons to accumulate at the surface of the insulating magnets during an exposure, an additional, conductive layer is spin coated on top of the PMMA. The insulating layer dissipates the electrostatic charges and is either aquaSAVE-53za bought from the Mitsubishi Chemical Corporation or Electra 92 from Allresist GmbH. Both of these products are water soluble, contrary to the PMMA layer, and can therefore easily be washed off after the exposure without damage to the PMMA layer. Similar to the PMMA layer, the conductive layer is spin coated at 4000 RPM for 90 s.

3. **Exposure**: Following the design of the resprective EBL step, a focused beam of electrons is scanned at the designated areas of the PMMA covered surface. To correlate the placement of the sample to the design, consecutive placement steps are to be followed. Firstly, the corners of the sample are located and marked by the 3-point correction method. Before the exposure, a focus, write field and aperture alignment procedure is executed to ensure a proper focus and overlap between the layers. Since most of the samples were cut by hand, the thicknesses of the samples can vary. In some cases, the z-coordinate had to be adjusted to remain within the focus range adjustable by the magnets.

   There are three EBL steps in order to optimize both the placement of different layers as well as providing a clean interface between the layers.

   (a) **Markers and big contact leads:** To avoid shifts between the steps, markers have to be placed. As a method to avoid exposing the surface while checking the proper location, the corners of the sample are flagged and correlated into the design. Then, the areas containing the markers and contact leads are exposed with an acceleration voltage of 30 kV and a dose of 400 μC m^{-2} in a Raith e-Line EBL system. These large areas are exposed with an aperture of 60 μm using a write field of 1000 μm by 1000 μm.
   In case of a large total area written with multiple structures, the contact pads were written in a larger aperture size of 120 μm to reduce the writing time.

   (b) **Pt Hall bar or strips:** The aperture of the smallest strip structure is chosen to be 10 μm with a so-called write field of 100 μm by 100 μm. The large Hall bar structures do not require such small aperture and the same parameters as for EBL step (a) is used.
   The 3-points correction method is used on the medium sized markers

while the smallest markers are aligned by a single image to ensure proper overlap between the layers within the range of ten nm.

(c) **Small contact leads:** In case of the non-local device geometry, a final step is performed where small leads are written. This has to be performed with a higher accuracy than can be achieved in EBL step (a) and thus requires the same settings as the Pt strips in EBL step (b). After this step, the exposed area is visible by microscope.

4. **Development:** Since the sample is covered by a water-soluble conductive layer, the sample is first submerged into a H_2O beaker for 30 s and blow dried with nitrogen. The development is done by a mixture of isapropanol (IPA) and methylisobutylketon (MIBK) with a ratio of 3:1. The exposed polymer chains are dissolved into the mixture while the unexposed parts remain intact. The sample is rinsed in a beaker of pure IPA to stop the development and blow dried with nitrogen.

5. **Deposition:** The contacts are deposited from Ti|Au by electron beam evaporation in a Temescal FC-2000 (TFC) at a base pressure of 10^{-4} Pa. The Ti increases the adhesion and has the side effect of lowering the pressure in the ultra-high vacuum system even before removing the shutter. A rate of 1Å/s is used for the Ti deposition. The Au has a low melting point and good conductivity properties and is deposited at a rate of 1Å/s for the first 5 nm after which the rate is ramped up to 3 Å/s with a final thickness of 75 nm. To ensure a proper conductivity at the small interface with Pt strips, an argon etch was performed for the small contact leads in the non-local geometry.

   The Pt is deposited by sputtering in a Kurt J. Lesker (KJL) sputter machine at a pressure of 3 10^{-1} Pa argon atmosphere. The rate is around 2 nm/s with a deposition time of 5 s and a power of 100 W. For some NiO devices, an argon etch is performed before the sputtering in the load lock at 200 W for 10 s. This improved the spin-mixing conductance by a factor of two as shown in Ch. 4. The evaporation method results in directional coverage on top of the PMMA and the magnet. The sputtering is unidirectional and therefore also covers the sides of the PMMA layer.

6. **Lift-off:** The remaining unexposed PMMA layer including the deposited material on top is removed by dissolving the PMMA layer in acetone of 48°C. In case of the coverage of Pt on the sides of the PMMA, the PMMA is less exposed to the acetone which can make the lift-of procedure more lengthy. Turbulence can be created by flushing with a pipet near the sample. Some mild sonication can also be used to get rid of metallic parts at unexposed areas.

- **Gluing and bonding:** When the sample is patterned, the sample has to be mounted on a chip carrier. Silver paste ensures a conductive connection to the chip carrier which has the upside for grounding the sample and using it as a back gate. The down side comes into play when re-using the sample as the silver particles can land on the top which are hard to get rid off. Therefore, most of the times, resin is used.
  For connecting the contacts to the measurement setup, wire bonding is performed on the contact pads. The wire, $Al_{0.99}Si_{0.01}$, is melted by sonication near the tip and can therefore be easily connected to the metal contact pads on one end and the chip carrier contact on the other end.

- **Mounting into the cryostat:** The chip carrier is mounted on a dipstick equipped with measurement wires and with an in-plane rotation degree of freedom. The dipstick is placed in a variable temperature insert (VTI) of a superconducting magnet cryostat which can produce magnetic fields up to $\mu_0 H = 7\,\mathrm{T}$ and temperatures in the range of [2 K– 300 K]. The helium flow is regulated by either an adaptive needle valve and in a later, optimised state of the cryostat, the variable pressure is regulated by a needle valve connecting the pump. To counter the cooling effect and allow fast temperature control, the heater of the heat exchanger is controlled by means of a proportional-integral-derivative (PID) feedback current. The inserted helium is heated to the required temperature.

3.3 Measurement setup

This section describes the measurement methods used to perform the work presented in this thesis. The working principle of the lock-in detection technique is explained, followed by a description of the measurement setups used for the experiments presented in this thesis.

The usage of four different Stanford research SR 830 lock-in amplifiers allows us to obtain both first and second harmonic responses of both the transverse and longitudinal probes in case of a Hall bar or both the local and the non-local probes in case of a non-local geometry. With the lock-in technique, the obtained AC signals are processed in order to optimize the signal-to-noise ratio.

A 'master' lock-in amplifier provides an AC voltage with angular frequency ω to a homebuilt so-called IV meetkast which turns the voltage into a current with the same frequency ω

$$I(t) = \sqrt{2} I_0 \sin(\omega t). \tag{3.1}$$

This current is lead through the sample via a switch box including a π-filter to diminish high-frequency components in the current and to protect the sample from current peaks. The signal has the form of an output voltage

$$V(t) = R_1 I(t) + R_2 I(t)^2 + R_3 I(t)^3 + R_4 I(t)^4 + R_5 I(t)^5 + ... \tag{3.2}$$

with $R_n I(t)^n$ being the nth order response. This voltage is amplified by the IV meetkast with a factor as high as possible to increase the signal-to-noise ratio. When a considerable background signal is present, which is the case og a longitudinal SMR measurement, the amplification factor needs to be reduced which lowers this signal-to-noise ratio.

The amplified signal is connected to one of the lock-in amplifiers where it is connected to the reference voltage frequency and phase of the 'master' lock-in amplifier, connected via the TTL port. The voltage component of frequency ω is the linear response and attributed to SMR in the local measurements and to electrically injected magnons in the case of a non-local measurement. The 2ω response of the signal voltage is related to heat effects and attributed to the SSE. For the purpose of measuring one of these effects, only the relevant frequency response is recorded and all the other frequencies are singled out from the output signal. The input signal and the reference signal are multiplied, resulting in a DC and AC voltage. The DC voltage is correlated to the reference and output voltage and is extracted by time averaging, the nth harmonic signal is obtained as

$$V^{nf} = \frac{\sqrt{2}}{T} \int_0^T \sin(n\omega t + \phi) V(t) dt \tag{3.3}$$

This could also be achieved by low-pass filtering the output signal.

In case of non-linear responses, for instance when the current bias is large, the nth-order response becomes a linear combination of V^{nf} which are

$$V^{1f} = R_1 I_0 + \frac{3}{2} R_3 I_0^3 + \frac{5}{2} R_5 I_0^5 + ... \tag{3.4}$$

$$V^{2f} = \frac{1}{\sqrt{2}} R_2 I_0^2 + \sqrt{2} R_4 I_0^4 + ... \tag{3.5}$$

$$V^{nf} = -\frac{1}{2} R_3 I_0^3 - \frac{4}{5} R_5 I_0^5 + ... \tag{3.6}$$

For the even orders, a phase shift of -90° is used. In this thesis, it is assumed that the higher order harmonics responses are considerably smaller than the first two, and are thus not taken into account. The same applies for the DC component of the current.

Bibliography

[1] N. Vlietstra, *Spin transport and dynamics in magnetic insulator/metal systems*, PhD thesis, Rijksuniversiteit Groningen, 2016.

[2] L. J. Cornelissen, *Magnon spin transport in magnetic insulators*, PhD thesis, Rijksuniversiteit Groningen, 2018.

[3] J. Shan, *Coupled charge, spin and heat transport in metal-insulator hybrid systems*, PhD thesis, Rijksuniversiteit Groningen, 2018.

[4] J. Liu, *Controlled magnon spin transport in insulating magnets*, PhD thesis, Rijksuniversiteit Groningen, 2019.

[5] N. Beaulieu, N. Kervarec, N. Thiery, O. Klein, V. Naletov, H. Hurdequint, G. De Loubens, J. B. Youssef, and N. Vukadinovic, "Temperature dependence of magnetic properties of a ultrathin yttrium-iron garnet film grown by liquid phase epitaxy: Effect of a Pt overlayer," *IEEE Magnetics Letters* **9**, pp. 1–5, 2018.